PHYSICAL REVIEW E VOLUME 49, NUMBER 6 JUNE 1994

# Transition to spatiotemporal chaos via spatially subharmonic oscillations of a periodic front

D. P. Vallette, W. S. Edwards, and J. P. Gollub
*Physics Department, Haverford College, Haverford, Pennsylvania 19041*
*and Physics Department, University of Pennsylvania, Philadelphia, Pennsylvania 19104*
(Received 28 February 1994)

An unusual sequence of bifurcations is documented in the flow of a viscous fluid inside a partially filled rotating horizontal cylinder. A periodic cellular pattern destabilizes to form a *spatially subharmonic* pattern that oscillates periodically in time. As the rotation rate is increased, the pattern evolves to spatiotemporal chaos. This state is characterized both by its correlation length and time, and by the fluctuating spatial phase of the pattern. The transition process is similar to that shown by a generalized Ginzburg-Landau model proposed by Daviaud *et al.* [Physica D **55**, 287 (1992)].

PACS number(s): 47.20.Lz, 47.52.+j, 47.54.+r

Secondary and higher bifurcations have been studied in several nonlinear systems that form patterns with stationary periodic ordering in one spatial dimension. These include Rayleigh-Bénard convection in an annulus [1,2], directional solidification [3,4], and directional viscous fingering [5,6]. Symmetry considerations indicate that these patterns may undergo a limited set of generic secondary bifurcations [7–9]. These include stationary bifurcations that break spatial symmetry, and oscillatory bifurcations that either break or retain spatial symmetry. Subsequent transitions to spatiotemporal chaos (STC) are characteristic of many of these systems. A number of experimental examples of STC have been recently reviewed by one of us [10]. Since the processes leading to STC are poorly understood, it is worthwhile to investigate them in detail.

This paper reports the observation of a type of bifurcation leading to spatiotemporal chaos that has apparently not been well documented: an instability of a periodic pattern that doubles the wavelength and leads to temporal oscillation. This phenomenon is revealed in the dynamics of a one-dimensional cellular front in the flow of a viscous fluid inside a rotating horizontal cylinder, sometimes termed rimming flow. The instability is one of several allowed by symmetry, as discussed by Coullet and Iooss [7]. (These generic instabilities may be classified according to the way in which perturbations of the stationary cellular pattern transform under time translation, space translation, and reflection.) The homogeneous oscillatory front undergoes a further transition to spatiotemporal chaos as the bifurcation parameter is increased. We analyze the transition using both correlation functions and complex demodulation, and compare the behavior to that observed in other systems.

A number of characteristic phenomena are observed in rimming flow. Melo and Douady [11] observed traveling solitary waves on a flat front that transformed continuously to a spatiotemporally chaotic state and subsequently to a periodic pattern as the angular velocity is increased. A cusped periodic front was previously reported by Johnson [12], who considered the difficult problem of the linear stability of the translationally symmetric front to perturbations along the axis of the cylinder. Other studies of rimming flows have identified an instability in which rings of fluid form into cells along the length of the cylinder, both in Newtonian fluids [13] and in viscoelastic fluids [14].

The experiment is described briefly in Fig. 1. Silicone oil of kinematic viscosity $\nu = 10$ cS (1 cS$\equiv 10^{-2}$ cm$^2$/s) flows inside a partially filled horizontal glass cylinder ($R = 5$ cm, $L = 50$ cm) which rotates about its axis at angular velocity $\Omega$. A thin layer of fluid coats the inner surface of the cylinder; excess fluid is dragged up the rising wall by viscosity and forms a thickened region of fluid that is stationary in the laboratory frame of reference. The azimuthal position $\Phi(x,t)$ of the lower edge of the thick region defines a horizontal front at axial position $x$ and time $t$, along the length of the cylinder. The cylinder is rotated by a computer controlled microstepping motor (4000 steps/revolution). Curvature of the front causes transmitted light to be refracted strongly; this allows convenient optical determination of $\Phi(x,t)$ in real time using a charge-coupled device (CCD) camera. The apparatus is placed inside a thermally insulated box and maintained at 25.5±0.3 °C to ensure uniform fluid properties.

Transitions observed in the behavior of the front are summarized in Fig. 2 at a fixed filling fraction [(fluid volume)/(cylinder volume)] $V = 0.0407$. (The effects of varying this parameter are mentioned later in this paper.) A single front is observed for angular velocities between

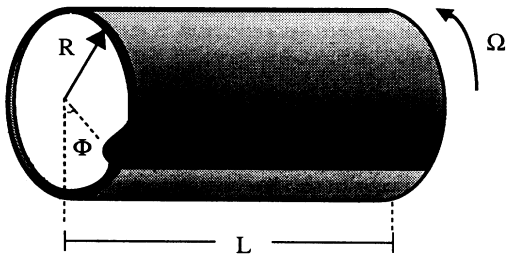


FIG. 1. Experimental apparatus. A horizontal glass cylinder is rotated about its axis at angular velocity $\Omega$. A small amount of oil coats the inner wall. Excess fluid forms a stable front at azimuthal position $\Phi(x,t)$ along the rising wall of the cylinder.

 

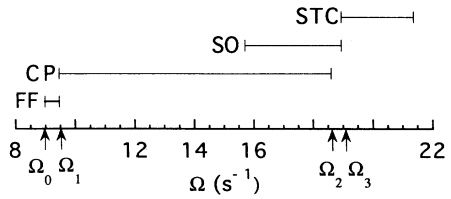


FIG. 2. Diagram of pattern transitions for $V = 0.0407$. The front position $\Phi(x,t)$ is defined in the range 8.98 $s^{-1} < \Omega < 21.4$ $s^{-1}$. (FF: flat front; CP: cellular pattern; SO: stationary oscillations; STC: spatiotemporal chaos.)

$\Omega_0 = 8.98$ $s^{-1}$ and $\Omega = 21.4$ $s^{-1}$. Below $\Omega_0$ fluid cascades continuously down the rising wall of the cylinder; above this range the front is pulled over the top of the cylinder. Just above $\Omega_0$ the front is flat along the length of the cylinder (labeled FF). It transforms supercritically to a cellular pattern (CP) at $\Omega_1 = 9.47$ $s^{-1}$, becoming strongly cusped as $\Omega$ increases. As $\Omega$ is increased quasistatically to $\Omega_2 = 18.60$ $s^{-1}$, the cusped peaks of the cellular pattern begin to oscillate vertically with a period $T_0 = 0.53$ s; neighboring peaks are 180° out of phase, so the spatial period has doubled. This state is denoted SO, for (spatially) subharmonic oscillations. The transition to oscillations is hysteretic with an overlap of $\Delta\Omega = 4.5$ $s^{-1}$, as indicated by the overlap between CP and SO in Fig. 2. Above $\Omega_3 = 18.94$ $s^{-1}$ the *spatial* phase of the base pattern and the oscillation amplitude begin to fluctuate in a continuous transition to spatiotemporal chaos. We have investigated this transition to spatiotemporal chaos as a function of the bifurcation parameter defined by $\mu = (\Omega - \Omega_2)/\Omega_2$.

The subharmonic oscillations of the cellular pattern (SO state) above $\mu = 0$ are seen in Fig. 3. The front position $\Phi(x)$ is plotted as a function of axial position, $x$, scaled by the pattern wavelength $\lambda = 0.98$ cm at onset of the oscillation. Successive fronts are displaced upward with time interval $0.2T_0$. The vertical scale of the front profile is the same as the horizontal scale. The sharp bends and flatness of the broad regions between cusps result from low vertical measurement resolution. The most pronounced feature in this state is the strong oscillation of the peaks in time; the broad flat portion of each cell remains stationary. The oscillations do not disrupt the spatial structure in the SO state.

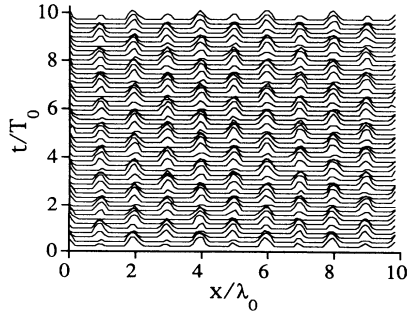


FIG. 3. Space-time plot of $\Phi(x,t_i)$ showing spatially period doubled oscillations. Times $t_i$ are displaced upward in $0.2T_0$ increments. [Bifurcation parameter $\mu = (\Omega - \Omega_2)/\Omega_2 = 0.0135$.]

As $\mu$ is increased above $\mu = 0.0183$ ($\Omega = \Omega_3$) spatial fluctuations emerge which disrupt the uniformity of the oscillating space-time pattern. A typical example of this state is shown in Fig. 4(a) for $\mu = 0.0220$. Here the front position $\Phi(x,t)$ is displayed in a gray scale, with darker regions corresponding to higher front positions (larger $\Phi$). The striations in the dark bands are due to the periodic front height oscillations that began in the SO state. In addition, we note *phase disturbances* of the cellular pattern that travel across the cylinder at a constant speed $\nu = 3.1$ cm/s. These are typically accompanied by a local reduction in the oscillation amplitude. The strength and frequency of these phase disturbances increase with $\mu$. At higher $\mu$, the pattern is often stretched or compressed sufficiently that a cell is created or annihilated. This event is accompanied by a localized burst of strong, rapid oscillations, further creation or annihilation events, and coherent displacements of the cellular pattern over several wavelengths [Fig. 4(b)]. This behavior is reminiscent of the intermittency observed in a variety of spatiotemporally evolving systems, in which chaotic events disrupt an otherwise ordered system [2,6,15]. However, here the chaotic fluctuations are clear, even in the absence of cell creation or annihilation events. The frequency of the bursts increases with increasing $\mu$ until they dominate the behavior.

The complex patterns may be characterized in part by their spatial and temporal correlation lengths $\xi(\mu)$ and $\tau(\mu)$, which are shown in nondimensional form in Fig. 5. These characteristic scales are defined by the decay of the

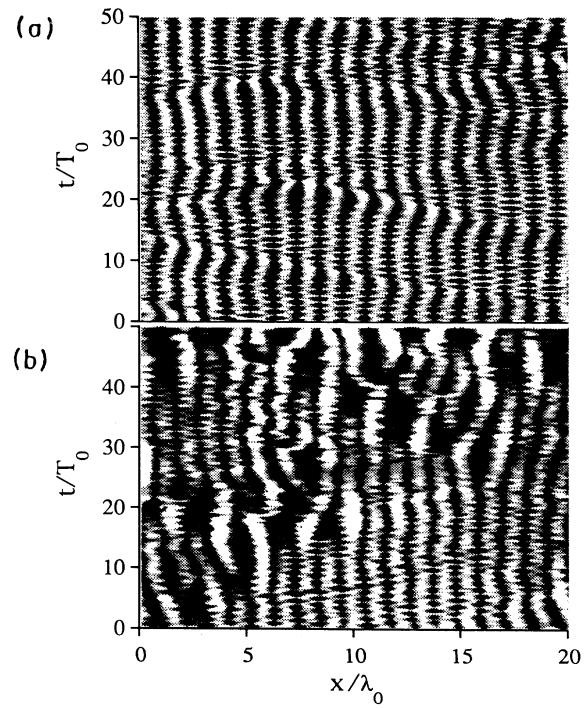


FIG. 4. Gray scale plots of $\Phi(x,t)$ at two values of $\mu$. (a) Localized fluctuations in the cellular structure propagate through the system at constant speed, accompanied by reduced oscillation amplitude, at $\mu = 0.0220$. (b) Bursts of nucleation and annihilation activity dominate the system in a saturated chaotic state at $\mu = 0.0487$.

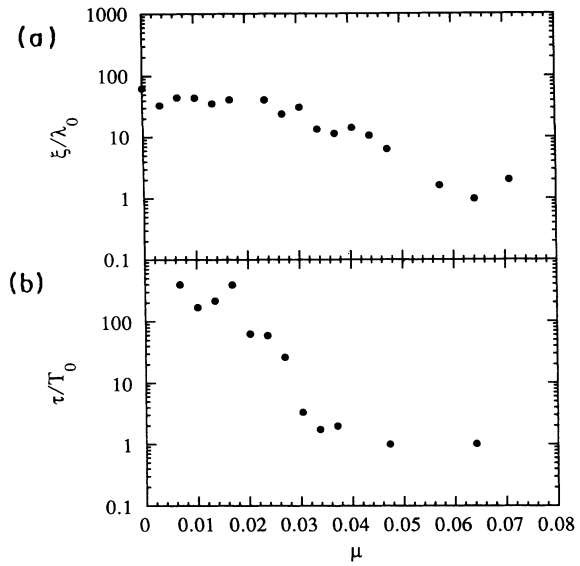


FIG. 5. Decrease of the nondimensional correlation length (a) and time (b) with increasing $\mu$.

autocorrelation function $C(x,t)$ in space and time [16]. The initial decline in $\tau/T_0$ is associated with the emergence of the traveling disturbances shown in Fig. 4(a). This process has less effect on $\xi/\lambda_0$, and the spatial correlation length does not begin to decrease strongly until the onset of bursting at about $\mu = 0.03$. When the spatiotemporal chaos is fully developed, $\tau/T_0$ and $\xi/\lambda_0$ are both comparable to unity. In some model systems [17], these two parameters decline following the same decay law as the bifurcation parameter is increased above the onset of STC. However, that is clearly not the case here.

A more complete picture of the range of phenomena shown by this system may be gained by noting the system's dependence on the filling fraction $V$. Below $V = 0.03$ cascading fluid is dragged directly over the top of the cylinder as $\Omega$ is increased. As a result, no stationary front can be defined. A flat front on which traveling waves may form is observed [11,18] for $V$ in the range $0.03 < V < 0.05$. When sufficiently dense, these traveling waves may form a stable cellular pattern, but it does not undergo the oscillatory bifurcation described in this paper. The stationary cellular pattern which undergoes the subharmonic oscillatory transition to chaos described here is observed for $V$ above 0.057. The critical angular velocities $\Omega_2$ and $\Omega_3$, and the wavelength $\lambda_0$ of the base pattern, all increase monotonically with $V$. We have not explored the behavior of the front for $V > 0.12$.

Since a full hydrodynamic description appears difficult, it is worth exploring the possibility of utilizing an amplitude equation for quantitative analysis. A possibly suitable generalized Ginzburg-Landau model has been studied numerically by Daviaud *et al.* [19]. It describes the long wavelength phase and amplitude fluctuations of an oscillating field that is coupled to a cellular pattern. These authors considered its applicability to the spatially periodic oscillatory state that occurs in nearly one-dimensional Rayleigh-Bénard (RB) convection. There are many qualitative similarities between the dynamical regimes exhibited by the two systems, though the oscillation in the present case is spatially subharmonic. The analysis of Daviaud *et al.* points out the utility of measuring the phase gradient of the cellular pattern. Linear stability analysis of the model equations demonstrated that the state of homogeneous oscillations may become unstable with respect to perturbations in the spatial phase of the cellular pattern; this destabilization is the result of a coupling between the oscillation amplitude and the phase gradient of the cellular pattern [19].

With these considerations in mind, we present in Fig. 6 a plot of the spatial phase gradient $\Gamma$ of the base pattern of Fig. 4(a). The phase is obtained by a demodulation of the complex Fourier transform $\tilde{\Phi}(k,\omega)$ about the wave number and frequency of the stationary cellular pattern ($k = 2\pi/\lambda_0, \omega = 0$). Dark regions correspond to stretching of the patter (small $\Gamma$) and light areas are regions of strong compression. These bands of large phase gradient appear to propagate with constant velocity. We also find that the subharmonic oscillation amplitude is reduced in the stretched regions (and vice versa). These experimental observations compare favorably with the simulation and experiments described in Ref. [19], in which nodes of zero oscillation amplitude are found to travel at constant speed above the onset of phase instability of the base pattern. Therefore it may be fruitful to explore the connection in greater detail, by actually measuring all of the relevant fluctuating fields: the phase of the base pattern (as shown in Fig. 5), and the complex oscillation amplitude. This work is in progress.

In summary, we observe a secondary instability of a cellular pattern to *spatially subharmonic oscillations.* This instability apparently breaks a different set of space-time symmetries from the set that is broken in other experiments [15]. The resulting oscillatory state undergoes a well defined transition to spatiotemporal chaos, marked by the emergence of fluctuations in the gradient of the phase of the cellular pattern. The loss of temporal coherence of the oscillations is coincident with the emergence

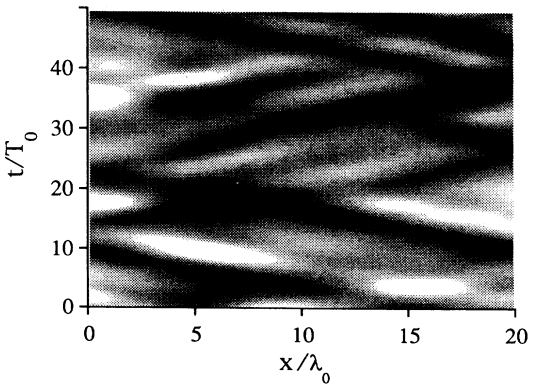


FIG. 6. Phase gradient of the cellular pattern obtained by demodulation of the structure in Fig. 4(a), for $\mu = 0.0220$. Dark regions correspond to pattern stretching and light regions to compression in this chaotic state.

of traveling bands of locally depressed or enhanced phase gradient. As seen elsewhere, spatial ordering is eventually lost as strong phase gradients lead to bursts of cell annihilation and nucleation. Studies of the dependence of these transitions on the filling fraction, and the detailed measurement and analysis of the fluctuating amplitude and phase fields, will be reported separately.

This work was supported by NSF Grant Nos. DMR-9319973 and CTS-9115005.

[1] F. Daviaud, M. Dubois, and P. Bergé, Europhys. Lett. **9**, 441 (1989).

[2] S. Ciliberto and P. Bigazzi, Phys. Rev. Lett. **60**, 286 (1988).

[3] A. J. Simon, J. Bechhoefer, and A. Libchaber, Phys. Rev. Lett. **61**, 2574 (1988).

[4] G. Faivre and J. Mergy, Phys. Rev. A **45**, 7320 (1992).

[5] M. Rabaud, S. Michalland, and Y. Couder, Phys. Rev. Lett. **64**, 184 (1990).

[6] S. Michalland, M. Rabaud, and Y. Couder, Europhys. Lett. **22**, 17 (1993).

[7] P. Coullet and G. Iooss, Phys. Rev. Lett. **64**, 866 (1990).

[8] J. D. Crawford and E. Knoblock, Annu. Rev. Fluid Mech. **23**, 341 (1991).

[9] R. E. Goldstein, G. H. Gunaratne, L. Gil, and P. Coullet, Phys. Rev. A **43**, 6700 (1991).

[10] J. P. Gollub, in *Turbulence, Weak and Strong*, edited by P. Tabeling (Plenum, New York, in press).

[11] F. Melo and S. Douady, Phys. Rev. Lett. **71**, 3283 (1993).

[12] R. E. Johnson, in *Engineering Science, Fluid Dynamics: A Symposium to Honor T. Y. Wu*, edited by G. T. Yates (World Scientific, Teaneck, NJ, 1990), p. 435.

[13] M. J. Karweit and S. Corrsin, Phys. Fluids **18**, 111 (1975).

[14] L. Preziosi and D. D. Joseph, J. Fluid Mech. **187**, 99 (1988).

[15] F. Daviaud, M. Bonetti, and M. Dubois, Phys. Rev. A **42**, 3388 (1990).

[16] A decaying exponential of characteristic length $\xi$ (or time $\tau$) is fitted to the envelope of the time (or space) average of $C(x,t)$. For a discussion of the use of correlation functions as tools for the analysis of STC see M. C. Cross and P. C. Hohenberg, Rev. Mod. Phys. **65**, 851 (1993).

[17] D. Hansel and H. Sompolinsky, Phys. Rev. Lett. **71**, 2710 (1993).

[18] F. Melo, Phys. Rev. E **48**, 2704 (1993).

[19] F. Daviaud, J. Lega, J. Bergé, P. Coullet, and M. Dubois, Physica D **55**, 287 (1992).

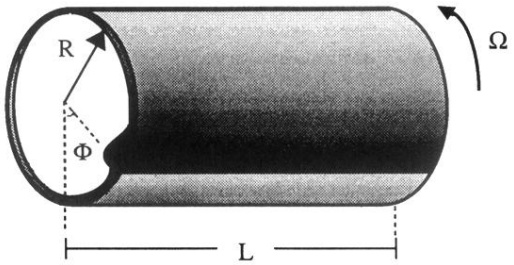


FIG. 1. Experimental apparatus. A horizontal glass cylinder is rotated about its axis at angular velocity $\Omega$. A small amount of oil coats the inner wall. Excess fluid forms a stable front at azimuthal position $\Phi(x,t)$ along the rising wall of the cylinder.

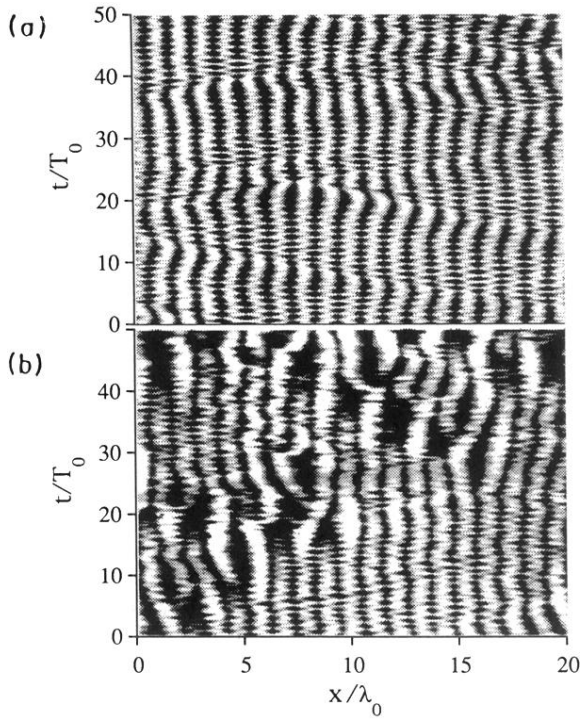


FIG. 4. Gray scale plots of $\Phi(x,t)$ at two values of $\mu$. (a) Localized fluctuations in the cellular structure propagate through the system at constant speed, accompanied by reduced oscillation amplitude, at $\mu = 0.0220$. (b) Bursts of nucleation and annihilation activity dominate the system in a saturated chaotic state at $\mu = 0.0487$.

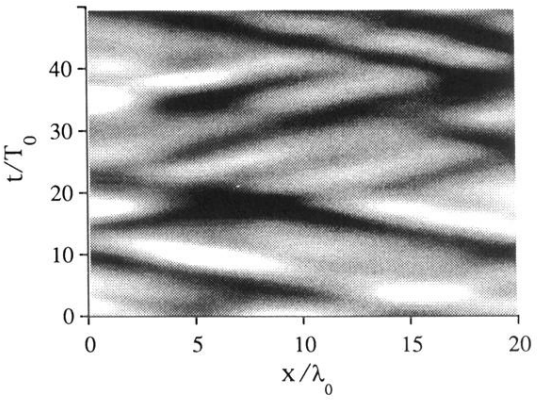


FIG. 6. Phase gradient of the cellular pattern obtained by demodulation of the structure in Fig. 4(a), for $\mu = 0.0220$. Dark regions correspond to pattern stretching and light regions to compression in this chaotic state.